

Analysis of Turing Patterns on a Spherical Surface Using Polyhedron Approximation

Takashi Yoshino

Department of Mechanical Engineering, Toyo University, Kujirai 2100, Kawagoe, Saitama 350-8585, Japan
E-mail address: tyoshino@toyo.jp

(Received June 12, 2016; Accepted February 16, 2017)

We considered Turing patterns on a spherical surface from the viewpoint of polyhedron geometry. We restrict our consideration to a set of parameters that produces a pattern of spots. We obtained numerical solutions for the Turing system on a spherical surface and approximated the solutions to convex polyhedrons. The polyhedron structure was dependent on both the radius of the sphere R and the initial condition. The number n of faces of the polyhedron increased with an increase in R . For small values of R , highly ordered structures were observed. With an increase of the value of R , a variety of structures were observed for each n , and the symmetry property of the spots, which determined the regularity of the polyhedron structure, gradually disappeared. We classified the numerical results according to their symmetrical properties of the approximated polyhedrons. The results revealed that the obtained Turing patterns lost symmetrical properties and varied the structures within same number of spots.

Key words: Turing Patterns, Spherical Surface, Polyhedron Approximation

1. Introduction

A Turing system [1] is a famous model in mathematical biology [2], and it is used to theoretically describe the morphogenesis of biological patterns. It consists of a couple of partial differential equations that describe the changes in concentrations of two chemical species, which are called the activator and the inhibitor. It is thought that this is the fundamental mechanism by which creatures are covered in patterns of spots or stripes [3]. The variety of patterns is thought to be caused by varying the reaction term and the values of the parameters.

Varea *et al.* [4] reported a model for a Turing pattern on a spherical surface. According to their paper, the patterns varied with the values of the parameters. They suggested that the variety of the spot patterns is related to the skeletal structure of spherical radiolaria, a kind of marine plankton [5]. In their paper, the structural properties of the obtained patterns were discussed for only a few cases. Therefore, a systematic consideration of the pattern structure is still required. In order to do this systematically, we introduce an approximation method that converts the patterns on a spherical surface to polyhedrons.

In a two-dimensional system, the spot patterns seem to be almost regular [6], and the pattern can be regarded as an optimized packing of equiradial disks on a plane [7]. Therefore, it is meaningful to compare a Turing pattern on a sphere with an optimized point configuration on a spherical surface. On the other hand, it is well known that Turing patterns depend on the initial conditions and size of domains [8]. The system size dependence causes

the existence of characteristic domain size of the Turing patterns. Callahan and Knobloch [9] revealed that patterns become less regular because many unstable modes exist and interact each other as the domain grows. It is not cleared yet how such dependences work on the spherical surfaces. The optimized configuration of a given number of points on sphere was discussed by Erber and Hockney [10]. For a given number of charged points on a sphere, they obtained the distribution that minimized the Coulomb energy of the system. For each number of points from 2 to 65, they summarized the fundamental properties such as the dipole moment, the Coulomb energy, the Coulomb angle, and the Tammes angle. Unfortunately, they did not discuss the symmetry property of the allocation of points over the whole sphere.

A polyhedron approximation using the Voronoi tessellation reveals features of the distribution of points on a spherical surface: the relationship between a set of spherical points and its regularity. The structure was obtained by a Voronoi tessellation on a spherical surface [11]. The shapes of the faces and the degrees of the vertices show how the points are allocated among the neighboring points. Also, the shape of the polyhedron shows intuitively the symmetrical properties of the allocation of the points. Recently, Yoshino [12] obtained the optimized point distribution on a spherical surface using the method of steepest descent (SD) and simulated annealing, and the results were then compared using a polyhedron approximation.

In this paper, we consider the distribution of spots in a Turing pattern on a spherical surface, using the corresponding polyhedron structure obtained from the distribution. In order to discuss this, we first calculate numerical solutions for a Turing system on a sphere. Next, we obtain the dis-

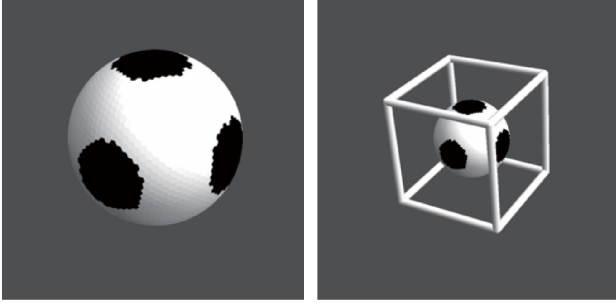


Fig. 1. An example of a binarized numerical solution and the corresponding approximated polyhedron ($R = 12.0$).

tribution of the centers of the spots and then use a Voronoi tessellation to approximate the patterns with polyhedrons. Finally, we discuss the basic properties and varieties of the polyhedron structures. Systematic classification of Turing pattern on the spherical surface is not carried out so that it is not clear how initial condition dependence and system size dependence affect the patterns.

2. Model

We considered the following Turing system [4, 6] consisting of concentrations of activator and inhibitor u and v , respectively:

$$\frac{\partial u}{\partial t} = D\delta\nabla^2 u + \alpha u(1 - r_1 v^2) + v(1 - r_2 u), \quad (1)$$

$$\frac{\partial v}{\partial t} = \delta\nabla^2 v + \beta \left(1 + \frac{\alpha r_1}{\beta} uv\right) + u(\gamma + r_2 v), \quad (2)$$

where δ is the diffusion coefficient of v and D is the ratio of the diffusion coefficient of u to that of v . The parameters α , β , γ , r_1 , and r_2 are for the chemical reactions. According to Turing [1], a difference in the diffusion constant between two chemical species produces a nonuniform pattern. In this study, D is taken to be smaller than 1, so that the chemical species corresponding to u diffuses slower than does the other species. The parameter δ is the characteristic diffusion constant.

We introduced new parameter R , defined from δ as $\delta = 1/R^2$. The parameter R corresponds to the system size, that is, the scaled radius of the sphere. If we scale Eqs. (1) and (2) with the substitutions $x \rightarrow Rx$, $y \rightarrow Ry$, and $z \rightarrow Rz$, the characteristic diffusion constant changes from δ to δ/R^2 . Therefore, an increase in δ corresponds to a decrease in the squared radius of the sphere. For this reason, we used the following equations instead of Eqs. (1) and (2):

$$\frac{\partial u}{\partial t} = \frac{D}{R^2}\nabla^2 u + \alpha u(1 - r_1 v^2) + v(1 - r_2 u), \quad (3)$$

$$\frac{\partial v}{\partial t} = \frac{1}{R^2}\nabla^2 v + \beta v \left(1 + \frac{\alpha r_1}{\beta} uv\right) + u(\gamma + r_2 v). \quad (4)$$

The method of that we used for our numerical simulation is summarized as follows: We used the fourth-order Runge-Kutta scheme. At the beginning of each simulation, the values of u and v were randomly allocated. The initial values were obtained from a uniform random generator and ranged from 0.0 to 0.005. We used “random()” function for

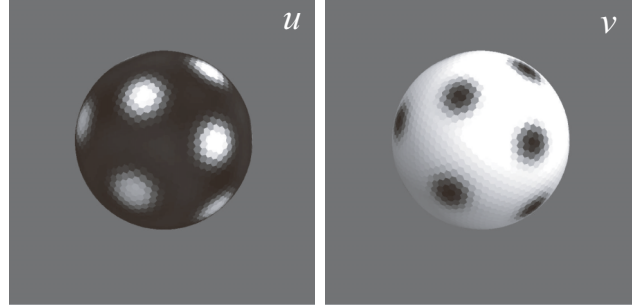


Fig. 2. An example of numerical solutions of u and v when $R = 12.0$.

standard C language library as random number generator. The period of the pseudo random number generation is estimated to $16(2^{31} - 1)$. The values of u and v at the same grid point were not correlated. The increase in time at each step was chosen to be $\Delta t = 0.01$. All simulations were carried out until the time t reached $t = 3,200$. For each value of R , we repeated the simulation ten times, each with a different seed.

We used a geodesic grid [13] for the numerical simulations. This grid was obtained from a triangular division of each face of a dodecahedron that was centered at the origin of the coordinates. All grid points were rescaled so that the distances of the grid points from the origin were all equal to unity. Therefore, the resolution of space was almost the same everywhere on the surface, and there was no singularity. We used a grid consisting of 2,562 vertices generated from the sixteen divisions of the edges of the dodecahedron.

We chose the values of the parameters of Eqs. (3) and (4) as follows: $D = 0.516$, $r_1 = 0.02$, $r_2 = 0.20$, $\alpha = 0.899$, $\beta = -0.91$, and $\gamma = -0.899$. These values were same as were used in one of the conditions of a previous study [4]. It is known that a pattern of spots arises when these parameter values are used. Note that our method of analysis, a polyhedron approximation, can be applied only to a spotted pattern.

We approximated the patterns of the numerical results to a frame structure that can be considered to be the edges of a convex polyhedron. The procedure for obtaining the approximating polyhedron is as follows: First, we binarized the values of v according to an appropriate threshold value; values greater than or equal to the threshold value were set to one, and those less than it were set to zero. As we will discuss below, the grid points assigned zero form spots. We calculated the center of each spot, and then we used these centers to carry out the Voronoi tessellation on the spherical surface [11, 12]. Finally, in order to construct the approximating polyhedron, we replaced the boundaries of the tessellation, which were arcs of great circles, with lines. Figure 1 shows an example of the correspondence between the binarized data and the approximating polyhedron. In this example, the number of spots was six, and the spot pattern was approximated as the frame of a cube.

We also considered the Coulomb energy and the Coulomb angle mentioned by Erber and Hockley [10]. Both of them characterize the distributions of points on a sphere. In order to calculate them, we used the centers of the spots

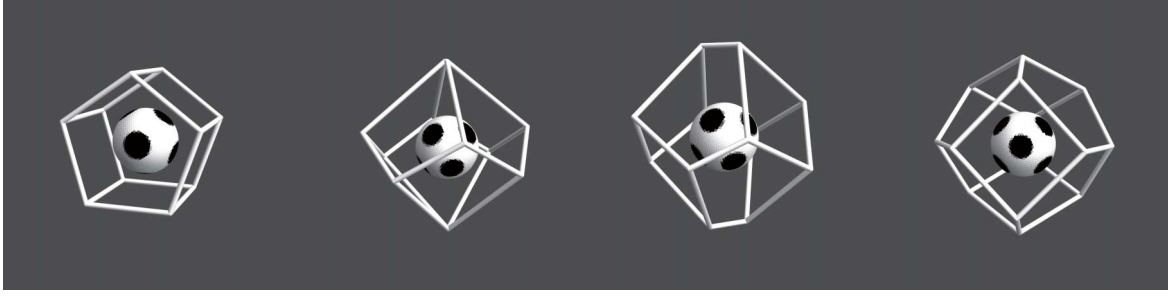
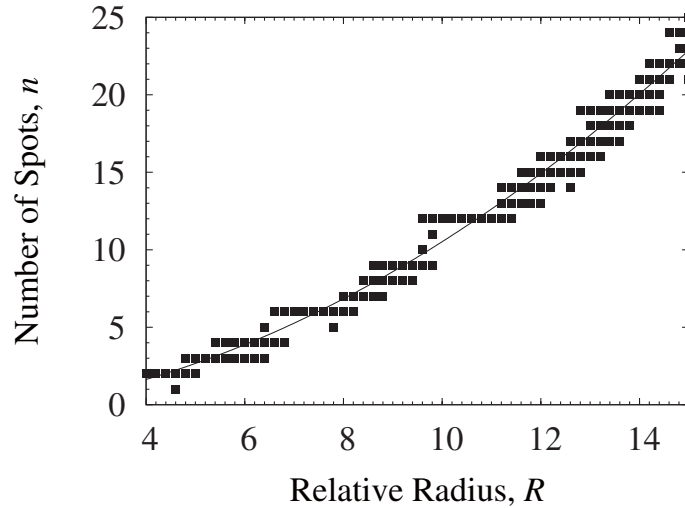
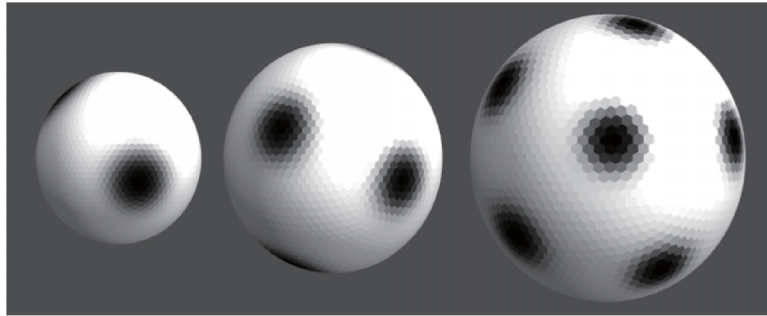
Fig. 3. Approximated polyhedrons for $R = 8.6$ with different initial conditions.

Fig. 4. Dependence of the number of spots on the relative radius.

Fig. 5. Examples of numerical solutions rescaled in order to be proportional to R . From left to right, the images correspond to $R = 6, 8$, and 10 .

that were obtained during the approximation procedure. The Coulomb energy E is defined by

$$E = \sum_{i=1}^{n-1} \sum_{j=i+1}^n \frac{1}{|\mathbf{r}_i - \mathbf{r}_j|}, \quad (5)$$

where \mathbf{r}_i is the position vector of the i -th center, and n is number of points on the sphere. The Coulomb angle is the minimum angular separation between pairs of points. The value is determined as the smallest value among the arccosines of the inner products of all pairs of points.

3. Results

The patterns of both u and v changed with time from the initial state and finally reached stable states. The ini-

tial random pattern changed gradually to a striped pattern, the stripes collapsed, and then spots formed. When R was larger, stable solutions were reached more rapidly than when R was smaller. Below, we will discuss the patterns at $t = 3, 200$, by which time all solutions were considered to be stable.

Figure 2 shows an example of Turing patterns on a spherical surface for $R = 12.0$. These patterns were obtained as stable solutions of u and v . The result are represented by a gray scale. The values are scaled according to a linear transformation for which the minimum value (zero) is black, and the maximum value (one) is white. The spherical surfaces were divided into polygons obtained from the Voronoi tessellation of the grid points. Each polygon was colored ac-

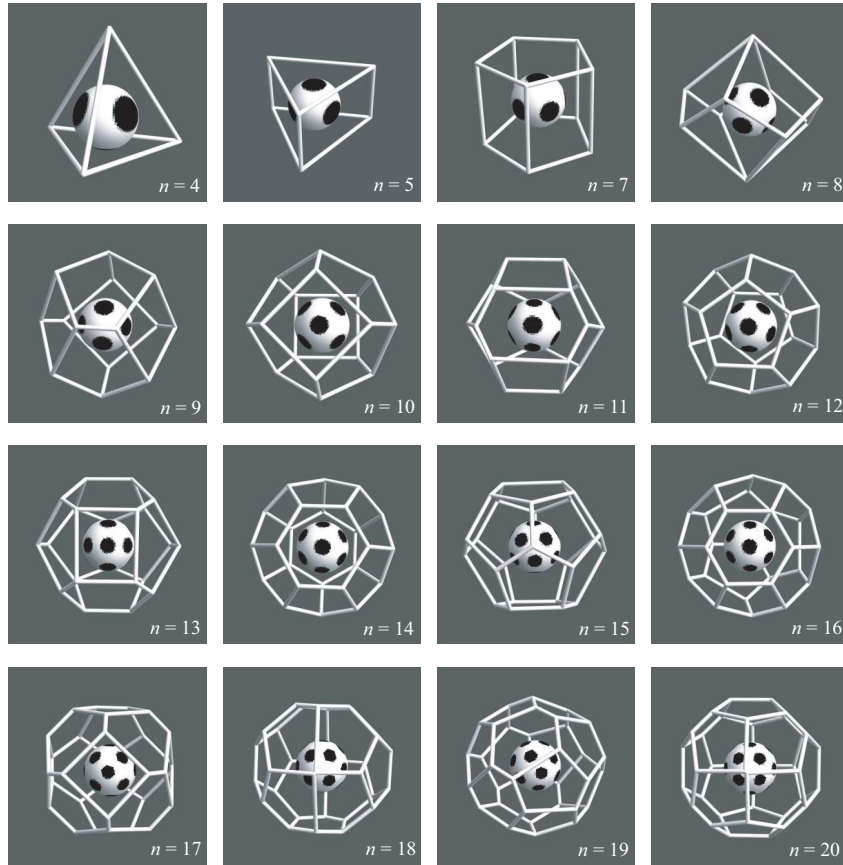


Fig. 6. Representative structures for each of n .

according to the value of the corresponding grid point. As shown in Fig. 2, in all cases, u and v were almost complementary, and so, in the following discussion, we will focus on the stable patterns of v .

Figure 3 shows the approximating polygons with stable patterns for $R = 8.6$ and obtained from four different initial conditions. The resulting patterns show four different structures, and these also have different numbers of spots: 7, 8, and 9. Similar differences with different initial conditions were frequently observed, especially in cases with larger values of R . Therefore, we conclude that the structure of the stable pattern is dependent on the initial conditions. For this reason, we tried ten simulations for each value of R , each with a different seed of random number generator.

The number of spots n was also dependent on R . We let the value of R range from 4 to 15 at intervals of 0.2. Figure 4 shows the R dependence of n . The value of n has a tendency to increase with an increase in R . The approximated curve shown in Fig. 4 was quadratic, and the formula estimated using the least-squares method was $n = 0.0902R^2 + 0.219R - 0.686$. Figure 5 shows a comparison of the stable patterns obtained using the different radii, which were proportional to R . For the same values of the parameters, the radii of the spots were approximately the same. This supports the conclusion that the relation between R and n is quadratic.

The approximating polyhedrons revealed in detail structural properties of the stable patterns. Figure 6 shows representative results for each value of n except for $n = 6$. The

result for $n = 6$ was shown in Fig. 1. For the representative structures, we chose the results for which the Coulomb energy had the smallest values for a given value of n . As n increases, the structure tends to be more complex and less ordered. For small values of R , we observed highly ordered patterns, regular polyhedrons. For $n = 4, 6$, and 12, the Platonic polyhedrons [14] were observed. We did not observe an octahedron ($n = 8$) or an icosahedron ($n = 20$). When $n = 8$, we observed a shape that was slightly different from an octahedron. Prisms, another kind of ordered structure, were observed for $n = 5, 6$, and 7. Other types of regular polyhedrons, such as Archimedes polyhedrons, were not observed.

Both the total number of vertices and the degrees of the vertices were dependent on n . When n was small, regular triangles and regular squares were frequently observed. On the other hand, when n was large, pentagons and hexagons were common. In many cases, they were almost equilateral or almost equiangular; however, irregular polygons were observed in some cases. A vertex of degree three was dominant in all cases except for a few cases with large R . In such cases, a vertex of degree four was observed.

Table 1 shows a summary of the basic properties of the representative results: the number of polygons; the number of i -gons for $i = 3, 4, 5$, and 6; the Coulomb energy; the Coulomb angle; the structural property of the polyhedron; and the number of other structures. We introduce the Schoenflies notation in order to summarize the symmetry properties of the various polyhedrons, and this is

Table 1. Summary of structural properties of representative patterns.

n	n_3	n_4	n_5	n_6	Coulomb energy	Coulomb angle (rad.)	Group	SD	Other structures
4	4	0	0	0	3.674	1.901	T _d	same	0
5	2	3	0	0	6.474	1.565	C _{3h}	same	0
6	0	6	0	0	9.986	1.550	O _h	same	0
7	0	5	2	0	14.454	1.252	C _{5h}	same	0
8	0	8	0	0	19.676	1.241	D _{4d}	same	1
9	0	3	6	0	25.762	1.193	D _{2h}	same	1
10	0	2	8	0	32.724	1.103	D _{4d}	same	0
11	0	2	8	1	40.612	1.005	C _{2v}	same	0
12	0	0	12	0	49.167	1.096	I _h	same	0
13	0	2	10	1	58.868	0.863	C _{2v}	same	1
14	0	0	12	2	69.317	0.912	D _{3d}	same	0
15	0	0	12	3	80.680	0.847	D _{3h}	different	1
16	0	0	12	4	92.920	0.839	C _{3v}	different	1
17	0	1	10	6	106.073	0.813	C _{2v}	different	3
18	0	0	16	2	120.377	0.774	C _{2v}	different	3
19	0	0	12	7	135.135	0.754	E	different	9
20	0	0	16	4	150.923	0.787	D _{4h}	same	4

listed in the ‘‘Group’’ column. We also include a comparison with the structure of the approximating polyhedron that was obtained from using the steepest descent method for the charged particles on a sphere, interacting through the Coulomb potential [12] in the ‘‘SD’’ column. We added short explanation of the steepest descent method in Appendix. Each row shows the values and representative results for each value of n . When n was large, different structures were observed for the same value of n . For this reason, we included a column titled ‘‘Other structures’’ in which we list the number of other structures observed. As mentioned above, we chose as representative the structure that had the smallest Coulomb energy. These also had the largest Coulomb angles. According to Euler’s polyhedron theory, n_5 is twelve if all the vertices are of degree three, and the faces are pentagons and hexagons. The values of n_5 for $n = 18$ and 20 were not twelve because there were vertices of degree four.

Both the Coulomb energies and the Coulomb angles of the representative structures were almost same as those with the optimized distribution of points on a sphere. In all cases, the differences were about 0.1% for the Coulomb energy and about 2% for the Coulomb angle. The values of the representative structures were greater than those of the optimized spherical point distributions for the Coulomb energies, but the reverse was true for the Coulomb angles.

The group theoretical notation of the structure shows that there is a tendency to lose structural order as n increases. For values of n from 15 to 19, structural similarities were not observed between these polyhedrons and those obtained from the optimized points. For $n = 20$, structural similarity is observed again.

4. Discussion

Polyhedron approximation is an effective method for recognizing the structural properties of the distribution of spots on the sphere. Our analysis revealed that the distribution of

spots is ordered, and it is highly dependent both on R and on the initial conditions. On the other hands, the disadvantage of this method is that the result is qualitative, and thus we cannot discuss the structural properties using numerical data. For example, we are unable to determine whether an obtained structure is optimized. In order to determine this, we have to introduce the qualitative criteria such as Coulomb energy and the Coulomb angle.

Although the obtained distributions of the centers of the spots were not optimized, the polyhedron structures nevertheless seemed to be sufficiently ordered. There were differences between the values of both the Coulomb energies and the Coulomb angles, and the values of these obtained using the method of the SD. In all cases, the values of the Coulomb energy of the spot patterns were larger than those of the spherical points from the SD, and the values of the Coulomb angles of the spot patterns were larger than those of the SD. This implies that the distribution of the centers is well ordered but is not optimized. Furthermore, the structural differences of the number of different structures in the cases of large R with that obtained from the SD support this estimation.

Some kind of repulsive effect seems to exist between the spots. With large values of n , the observed polyhedron structures were not symmetric, and this differs from what was observed with the coulomb interaction. The variety of structures observed for large values of n are thought to be due to the absence of an ordered configuration on the sphere itself and to an interacting effect between the spots.

The introduction of group theoretical notation is useful for classification of the spot patterns on a sphere. This is because we cannot see the whole area from any viewpoint. The notation enables us to summarize the properties of the patterns.

The reason there is a variety of skeletal structures for spherical radiolaria is that the stable patterns depend on both R and the initial conditions; their shapes depend on

their radii and the initial concentrations of the key chemical species. Slight differences in R or the initial conditions can result in different patterns of spots and different skeletal structures of spherical radiolaria.

Acknowledgments. This research was supported by the Ministry of Education, Science, Sports, and Culture, Grant-in-Aid, No. 23560074 and No. 16K05045. The author would like to thank Prof. A. Matsuoka of Niigata University for his comment on the variety of skeletal structures of spherical radiolaria.

Appendix A.

The steepest descend (SD) is widely used for optimization problem. This method brings us the local minimum configuration of the variables. The procedure uses the forces acting on the points on a sphere. We denote the position of the i -th point $\mathbf{r}_i = (x_i, y_i, z_i)$. A repulsive force acting on the i -th point \mathbf{F}_i is calculated by,

$$\mathbf{F}_i = -\nabla_i E,$$

where $\nabla_i \equiv (\partial/\partial x_i, \partial/\partial y_i, \partial/\partial z_i)$ and E is defined in Eq. (5). In the steepest descent method, the variables are changed in accordance with the force to minimize the potential. After enough repeat of the changes, the points reach static configuration which locally minimize its potential energy. The detailed description is found in Yoshino [12].

References

- [1] A. M. Turing, The chemical basis of morphogenesis, *Philosophical Transactions of the Royal Society of London. Series B*, **237** (1952), 37–72.
- [2] J. Murray, *Mathematical Biology II: Spatial Models and Biomedical Applications*, 3rd ed., Springer-Verlag, Berlin Heidelberg, 2003.
- [3] S. Kondo and T. Miura, Reaction-diffusion model as a framework for understanding biological pattern formation, *Science*, **329** (2010), 1616–1620.
- [4] C. Varea, J. L. Aragon, and R. A. Barrio, *Physical Review*, **E60** (1999), 4588–4592.
- [5] P. De Wever, P. Dumitrica, J. Caulet, C. Nigrini, and M. Caridroit, *Radiolarians in the Sedimentary Record*, Gordon and Breach Science Publishers, Amsterdam, 2001.
- [6] R. A. Barrio, C. Varea, J. L. Aragon, and P. K. Maini, A two-dimensional numerical study of spatial pattern formation in interacting turing systems, *Bulletin of Mathematical Biology*, **61** (1999), 483–505.
- [7] S. Torquato and F. H. Stillinger, *Reviews of Modern Physics*, **82** (2010), 2633–2672.
- [8] E. J. Crampin, E. A. Gaffney, and P. K. Maini, *Bulletin of Mathematical Biology*, **61** (1999), 1093–1120.
- [9] T. K. Callahan and E. Knobloch, *Physica D*, **132** (1999), 339–362.
- [10] T. Erber and G. M. Hockney, *Journal of Physics A: Mathematical and General*, **24** (1991), L1369–L1377.
- [11] A. Okabe, B. Boots, K. Sugihara, and S. N. Chiu, *Spatial Tessellations: Concepts and Applications of Voronoi Diagrams*, 2nd ed., John Wiley & Sons, Chichester, 2000.
- [12] T. Yoshino, Symmetry properties of results of a geometrical modelling method of radiolarian skeleton, *Symmetry: Culture and Science*, **24** (2013), 175–183.
- [13] R. Sadourny, A. Arakawa, and Y. Mintz, *Monthly Weather Review*, **96** (1968), 351–356.
- [14] H. S. M. Coxeter, *Regular Polytopes*, Dover Publications, New York, 1973.